Journal of Applied Polymer Science

Resorcinol formaldehyde xerogels modified with mercapto functional groups as mercury adsorbent

Siamak Motahari, Behzad Shiroud Heidari, Ghodratollah Hashemi Motlagh
School of Chemical Engineering, Faculty of Engineering, University of Tehran, P. O. Box: 11365/4563, Tehran, Iran
Correspondence to: S. Motahari (E-mail: Mosmotahari@ut.ac.ir)

ABSTRACT: Resorcinol formaldehyde xerogels are modified by mercaptopropyl-trimethoxysilane during the sol–gel process used to produce the xerogel. The chemical modification is confirmed by Fourier-transform infrared spectroscopy. The xerogel is then used to adsorb mercury ions from aqueous solutions. The effects of the molar ratios of the precursors as well as the catalyst and the modifier are studied on the textural properties of the xerogel and the adsorption efficiency. It is shown that the chemical modification of the resorcinol formaldehyde xerogels creates the chemical sites on the structure of the xerogel to adsorb more mercury ions and increase the adsorption efficiency. At the same time, chemical modification decreases the xerogel surface area which results in a reduction of the mercury adsorption. Therefore, there exists an optimum value for the chemical modification of the xerogel to achieve the highest adsorption efficiency. Adsorption kinetics as well as equilibrium isotherm of xerogels were examined using pseudo-first- and second-order kinetic equations, and Freundlich and Langmuir isotherm models. The adsorption kinetics was found to follow the pseudo-second-order kinetic equations. The experimental data was also fitted into the Longmuir model more precisely comparing the Freundlich model. Finally, a series of mercury adsorption–desorption tests proved that the optimized mercapto-modified resorcinol formaldehyde xerogel was an efficient reusable adsorbent for mercury ions. © 2015 Wiley Periodicals, Inc. J. Appl. Polym. Sci. **2015**, *132*, 42543.

KEYWORDS: adsorption; gels; polycondensation; surfaces and interfaces

Received 15 March 2015; accepted 26 May 2015
DOI: 10.1002/app.42543

INTRODUCTION

Mercury is one of the most toxic contaminants among heavy metal ions which have been classified by the United States Environmental Protection Agency (US EPA) and European Union (EU) as a priority pollutant.[1,2] The major sources of mercury pollution are industries.[3] Because of the development of industries and toxic effects of mercury on human health, it has been necessary to remove this pollutant from industrial effluents before releasing it into the environment. The adsorption process, as a technique for mercury removal, has been found to be appropriate with advantages such as easy performance and high efficiency even at low concentrations.[4–6] However, the efficiency of this process mainly depends on the physical and chemical structure of the adsorbents.

Resorcinol-formaldehyde (RF) gels are a kind of nanoporous organic materials which are prepared by sol–gel polycondensation reaction. These gels because of their unique properties, such as low density, high surface area, and high porosity, have many applications for super capacitors, heat insulators, catalyst supports, and adsorption materials.[7–10]

Physical properties of the pore structure like surface area, pore volume, and pore size distribution (PSD) are drastically altered by different synthesis conditions. The initial gel pH and the resorcinol-to-catalyst ratio of the RF solution are important synthesis factors that affect the structural properties of the RF gels.[11–17] The effect of different chemical catalysts on the gel properties is believed to be due to their effect on the pH of the precursor solution.[17] This means that the effect of basic or acidic catalysts depends mainly on the acidic or basic effect of the catalyst itself.[18] Herein, Job *et al.* reported that sodium carbonate is not actually a catalyst; in other words, it has only a primary role in increasing the initial pH of the solution by increasing the OH^-/H^+ ratio.[19] They also found that as pH decreases, mesopores become wider and tend to form macroporous structures. Lin and Ritter controlled the pore texture of carbon xerogels by varying the initial pH in the range of 5.5–7.5. In that work, xerogels exhibited the highest surface area and pore volume between an initial pH of 5.5 and 6.0 and when the pH increased from 6.5 to 7.0, the surface area suddenly decreased to a minimum value.[20]

Pore surface chemistry, as well as the physical properties of pore structure, is the major factor in the adsorption process.[21]

Functionalized porous adsorbents have been widely used for selective metal removal from an aqueous medium. In the specific case of mercury selective adsorption, thiol-functionalized mesoporous materials have been of interest in the last decade due to the high chemical attraction of sulfur groups toward mercury.[22–24] The importance of having metal-binding functional groups, e.g., —SH, at the aerogel pore surface was realized by Štandeker *et al.* who functionalized a novel series of silica aerogels with mercaptopropyl-trimethoxysilane (MPTMS) using a sol–gel synthesis.[25] They found that by increasing the amount of MPTMS in silica aerogels, the specific surface area, pore volume, and average pore size decrease because co-hydrolysis of MPTMS and silane precursor (tetramethoxysilane) proceeds one after another and unwanted organosilane polymerization occurs, although, the modifications improved adsorption efficiency in the all modified aerogels. Faghihian *et al.* obtained compatible results, as they reported that using amino-propyl-triethoxysilane for modifying silica aerogels corresponded to a substantial reduction in the specific surface area after modification.[26]

To the best knowledge of the authors, no investigation and optimization on the synthesis of RF gels modified with mercapto functional groups used for heavy metal adsorption have been reported yet. Therefore, the aim of this study is to optimize the structural properties of functionalized RF gels for mercury adsorption. For this purpose, the synthesis factors such as the resorcinol–catalyst ratio and the amount of mercapto functional groups in RF solution are varied to achieve the optimized RF gel as an adsorbent. In this work, the ambient drying method[11] is used to produce low-cost adsorbent. Meanwhile, the RF xerogels are characterized by Fourier transform infrared (FTIR) spectra, nitrogen physisorption, scanning electron microscopy (SEM), and thermogravimetric analysis (TGA) and also the adsorption performance of xerogels is studied by flame atomic absorption spectrophotometer (FAAS). In this study, mercury adsorption isotherm and kinetics are investigated by applying different models for the optimized mercapto-modified and unmodified RF xerogels. The adsorption–desorption cycle is also repeated five times to evaluate the reusability of the optimized mercapto-modified adsorbent.

EXPERIMENTAL

Chemicals and Reagents

The materials used for the preparation of RF xerogels were resorcinol (98%, Aldrich), formaldehyde (37% in water, Merck), and mercaptopropyl-trimethoxysilane (97%, Merck) as the modifier. The other chemicals included magnesium sulfate heptahydrate (99%, ACS) as the catalyst, distilled water, and acetone as solvents.

For adsorption tests, a synthetic stock solution of mercury ions was prepared by dissolving the required quantity of mercury (II) nitrate monohydrate (ACS) in distilled demineralized water and pH adjustment were performed by 0.1 M HNO_3 or 0.1 M NaOH when necessary.

Adsorbent Preparation

RF xerogel adsorbents were prepared by a polycondensation reaction between resorcinol (R) and formaldehyde (F) according to the sol–gel synthesis proposed by Pekala *et al.*,[27] and the modification occurred by adding mercaptopropyl-trimethoxysilane (MPTMS) during the synthesis stage. In contrast to the conventional method, where sodium carbonate (Na_2CO_3) is used as a basic catalyst, magnesium sulfate heptahydrate ($MgSO_4{\cdot}7H_2O$) was used as a weak acidic catalyst (C). The RF solutions were prepared by changing the resorcinol-to-catalyst molar ratio (*R/C*) and the ratio of MPTMS to resorcinol (*M/R*). Also, the resorcinol-to-formaldehyde molar ratio (*R/F*) and the dilution ratio (water/(resorcinol + formaldehyde + catalyst + MPTMS) molar ratio) were fixed at 0.5 and 6, respectively. After adding R and F to the water–catalyst solution, the sealed solution was magnetically stirred for 10 min. Then MPTMS was slowly added to the solution. The solution was stirred continuously for 15 min, then decanted into glass vials and cured for 24 h at 25°C followed by 24 h at 50°C and 72 h at 85°C. At the end of the gelation/aging step, the wet gel was treated with pure acetone in a bath for 72 h at 30°C to exchange the pore liquid. The fresh acetone was replaced daily to remove the residual water that had entered the bath during the solvent exchange process. Finally, the sample was dried at 35°C for 24 h. Figure 1 shows the synthesis procedure of the modified RF xerogel.

To study the influence of the synthesis parameters on the porous properties and adsorption process, the amounts of MPTMS and catalyst were changed. Table I presents the materials and their ratios for each sample. As shown in the table, the amounts of water were slightly changed in some samples to fix the value of the dilution ratio (*D*) at 6. The synthesized xerogels were named as RC"X"-M"Y" that "X" and "Y" showed *R/C* and M/R molar ratio, respectively. For example, RC50-M0.24 indicated the sample prepared by R/C = 50 and M/R = 0.24. RC1000-Pure corresponded to the unmodified sample. Meanwhile, in this article, the "optimized mercapto-modified RF xerogel" refers to the modified xerogel that has the highest adsorption efficiency.

Adsorbent Characterization

Chemical modifications of RF xerogels were investigated by FTIR spectra (Bruker Tensor 27, Bruker Optics Inc., Germany) which provided information about the chemical and functional group bonds. The FTIR spectra were acquired from 64 scans with a 2 cm^{-1} resolution in the range of 400–4000 cm^{-1} and using KBr disks. Morphology of the adsorbent was studied by scanning electron microscopy (SEM) (AIS2100, Seron Technology, Korea) which was performed on gold-coated samples at an accelerating voltage of 15 kV.

The pore texture of the adsorbents was characterized by nitrogen physisorption at 77 K using an automatic adsorption and desorption apparatus (BEL sorp-mini II, BEL Japan Inc., Japan). All samples were heated at 383 K in a vacuum for 2 h prior to measurement. The specific surface areas (S_{BET}) and micropore volumes (V_{mic}) were evaluated based on the Brunauer–Emmet–Teller (BET) theory[28] and *t*-plot analysis,[29] respectively. The Barrett–Johner–Halender (BJH) method[30] was used to calculate the PSD and the mesopore volume (V_{mes}) of the xerogels.

To investigate the effect of chemical modification on the thermal stability of the xerogels, thermogravimetry (TG) analysis

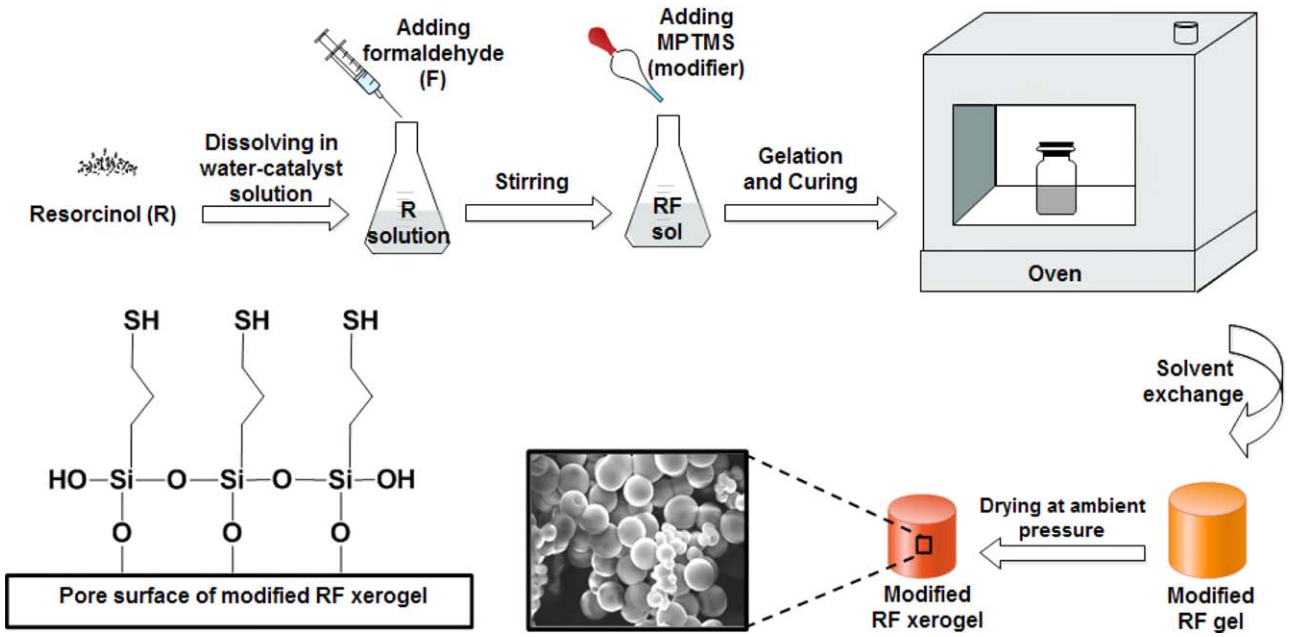

Figure 1. Schematic illustration of synthesis procedure of modified RF xerogels. [Color figure can be viewed in the online issue, which is available at wileyonlinelibrary.com.]

was performed using a thermogravimetric Analyzer (TGA-50H thermobalance, Shimadzu Inc., Japan). The measurements were conducted under nitrogen atmosphere over a temperature range of 25–900°C at a scan rate of 10°C min^{-1}.

Adsorption Experiments

The adsorption of mercury ions (Hg(II)) on xerogels was studied by batch technique.[3] A stock solution of Hg(II) with a concentration of 500 mg L^{-1} was prepared by diluting mercury (II) nitrate monohydrate in distilled water and it was then diluted to make the purpose solution for each experiment. Then, a certain amount of adsorbent, e.g., 0.15 g, was added to 100 mL of diluted solution in a conical flask to achieve a certain adsorbent dose, e.g., 1.5 g L^{-1}. Then the suspension was magnetically stirred at 25°C for a predetermined period of time. After equilibration, the suspension was filtered and analyzed by a flame atomic absorption spectrophotometer (FAAS) (Analyst 200, Perkin-Elmer Instruments, USA). This procedure was carried out for the adsorption studies of all synthesized xerogels. The adsorption efficiencies and capacities were calculated using eqs. (1) and (2), respectively:

$$E = \frac{C_0 - C_e}{C_0} \times 100 \quad (1)$$

$$q_e = \frac{(C_0 - C_e)}{m} V \quad (2)$$

Where E is the Hg(II) removal percentage, q_e is the quantity of mercury adsorbed, C_0 and C_e are the initial and equilibrium liquid-phase concentration of Hg(II), respectively, V is the volume of the diluted mercury(II) nitrate solution, and m is the dry mass of the adsorbent used.

After comparing the adsorption results for all synthesized xerogels, the optimized mercapto-modified RF xerogel, which

Table I. Formulations of Xerogel Samples

				Precursors (mol)				
Sample	*R*/*C* (mol/mol)	*M*/*R* (mol/mol)	*D* (mol/mol)	*R*	*F*	*C*	*M*	*W*
RC50-M0.24	50	0.24	6	0.123	0.246	0.0024	0.030	2.7
RC200-M0.24	200	0.24	6	0.123	0.246	0.0012	0.030	2.7
RC600-M0.24	600	0.24	6	0.123	0.246	0.0006	0.030	2.7
RC1000-M0.24[a]	1000	0.24	6	0.123	0.246	0.0003	0.030	2.7
RC1000-Pure	1000	0	6	0.123	0.246	0.0003	0	2.5
RC1000-M0.12	1000	0.12	6	0.123	0.246	0.0003	0.015	2.6
RC1000-M0.24[a]	1000	0.24	6	0.123	0.246	0.0003	0.030	2.7
RC1000-M0.48	1000	0.48	6	0.123	0.246	0.0003	0.060	2.9
RC1000-M0.72	1000	0.72	6	0.123	0.246	0.0003	0.090	3.1

[a] Same sample.

showed the highest adsorption efficiency, was determined. Then, the effects of several parameters such as contact time, initial Hg(II) concentration, and pH on the adsorption efficiency were studied only for the optimized mercapto-modified and unmodified RF xerogels. It should be noted that the effect of contact time and initial Hg(II) concentration were only investigated for the study of adsorption isotherm and kinetics, respectively. Thus, for the sake of conciseness, these effects are not reported in this article.

Adsorption Isotherm

An adsorption isotherm is characterized by certain constant values, which express the surface properties and affinity of the adsorbent and can also be used to optimize the use of adsorbent. Several mathematical models can be used to describe the experimental data of the adsorption isotherms.[31] Langmuir and Freundlich isotherm equations have been examined in this study.

Langmuir Isotherm. The Langmuir isotherm assumes that adsorption takes place at specific homogenous sites within the adsorbent and models the monolayer adsorption processes.[32] The linearized equation of the Langmuir model is given as follows:

$$\frac{C_e}{q_e}=\frac{C_e}{q_m}+\frac{1}{K_L q_m} \tag{3}$$

Where q_e (mg g^{-1}) is the amount of the metal ions adsorbed per unit mass of the adsorbent at equilibrium state; C_e (mg L^{-1}) is the equilibrium concentration; q_m (mg g^{-1}) and K_L (L mg^{-1}) are Langmuir constants related to the theoretical monolayer adsorption capacity and the energy of adsorption, respectively. The parameters q_m and K_L can be calculated from the slope and the intercept of the linear plot of C_e/q_e *vs* C_e.

The essential feature of the Langmuir isotherm can be expressed by means of a dimensionless equilibrium parameter (R_L), which is defined as:

$$R_L=\frac{1}{1+C_0 K_L} \tag{4}$$

Where K_L (L mg^{-1}) is the Langmuir constant and C_0 (mg L^{-1}) is the highest Hg(II) concentration. The value of R_L indicates the type of the isotherm to be either unfavorable ($R_L > 1$), linear ($R_L = 1$), favorable ($0 < R_L < 1$) or irreversible ($R_L = 0$).[25]

Freundlich Isotherm. The Freundlich isotherm describes a multilayer adsorption, with a nonuniform distribution of adsorption heat and affinities over the heterogeneous surface.[33] This empirical model is represented by eq. (5):

$$q_e=K_F C_e^{1/n} \tag{5}$$

Where q_e (mg g^{-1}) is the same as explained in the last section, n is the energetic heterogeneity factor of the adsorption surface, and K_F is the Freundlich constant which can be defined as the adsorption or distribution coefficient and expresses the amount of ions adsorbed onto adsorbent for a unit equilibrium concentration.[34] The linearized form of the Freundlich model is given by the following equation:

$$\log q_e=\log K_F+\frac{1}{n}\log C_e \tag{6}$$

Where n and K_F can be obtained from the slope and intercept of the linear plot of log q_e *vs* log C_e, respectively.

Adsorption Kinetics

In order to explain the adsorption process of Hg(II) on xerogels, the adsorption kinetics are investigated. A pseudo-first-order kinetics model and a pseudo-second-order kinetics model are applied for the adsorption of mercury ions on the xerogels.

Pseudo-First-Order Kinetics Model. The integral form of pseudo-first-order kinetics model is expressed as follows:[31]

$$\log(q_e-q_t)=\log q_e-\frac{k_1}{2.303}t \tag{7}$$

Where q_e and q_t (both in mg g^{-1}) are the adsorption capacity of Hg(II) at equilibrium and at time t (min), respectively, and k_1 (min^{-1}) is the rate constant of pseudo-first-order adsorption.

Pseudo-Second-Order Kinetics Model. The adsorption kinetics may also be described by a pseudo-second-order reaction. The linearized-integral form of pseudo-second-order kinetics model is:[31]

$$\frac{t}{q_t}=\frac{t}{q_e}+\frac{1}{k_2 q_e^2} \tag{8}$$

Where q_e and q_t have the same definition as explained in the last section, and k_2 (g mg^{-1} min^{-1}) is the pseudo-second-order rate constant.

Desorption of Hg(II) and Adsorbent Reuse

To study the desorption performance, 1.5 g of optimized mercapto-modified was added to 50 mL Hg(II) solution (50 mg L^{-1}). When the adsorption was completed, the suspension was centrifuged and the collected xerogels were washed with deionized water several times to remove residual Hg(II) on the surface. Then the xerogel was transferred to a container holding 50 mL of 3M HCl containing 2% (m/v) thiourea as the desorbent agent. The suspension was shaken by a mechanical shaker for 3 h at 25°C, then the filtrate was analyzed by FASS to determine the concentration of Hg(II) after desorption. To investigate the reusability of the adsorbent, the modified RF xerogel was then reused in another adsorption experiment in the same way as the first time. The adsorption–desorption cycle was repeated five times.

Desorption ratio was calculated using eq. (9):

$$D=\frac{M_{des}}{M_{ads}}\times 100 \tag{9}$$

Where D (%) is the desorption ratio, M_{des} (mg) is the amount of Hg(II) ions desorbed in the desorbent agent, and M_{ads} (mg) is the amount of Hg(II) ions adsorbed on the modified xerogel.

RESULTS AND DISCUSSION

Adsorbent Characterization

FTIR Analysis. The FTIR spectra of RC1000-Pure, RC1000-M0.12, RC1000-M0.24, and RC1000-M0.48 indicate bonds corresponding to the networks structural units (Figure 2). The broad absorption band at 3422 cm^{-1} is attributed to —OH stretching vibrations of aromatic ring hydroxyl groups and

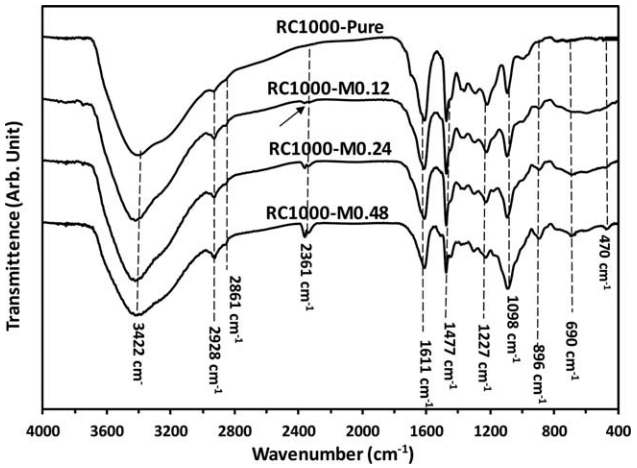

Figure 2. FTIR spectra of RC1000-Pure, RC1000-M0.12, RC1000-M0.24, and RC1000-M0.48.

some silanol (Si—OH) groups.[27,35] The absorption bands at 2928, 2861, and 1477 cm^{-1} are the characteristic of C—H stretching and bending vibrations of MPTMS and methylene bridges between aromatic rings.[27] Comparing the spectra of the samples indicates the C—H peaks (in 2928 and 2861 cm^{-1}) become stronger with increasing *M*/*R* ratio due to propyl groups in the modifier. The IR absorption band at 1614 cm^{-1} is assigned to aromatic ring stretching vibrations. The IR bands at 1227 and 1098 cm^{-1} are characteristic of C—O—C stretching vibrations of methylene ether bridges among resorcinol molecules,[27] but with increasing *M*/*R* ratio in the samples, the peak in 1227 cm^{-1} becomes weaker because of the C—O—C bond being converted to siloxane groups located among the aromatic rings. This replacement causes the peaks at 1098 cm^{-1} to become sharper due to the presence of asymmetric Si—O—Si and Si—O—C bonds (C can be attributed to benzene ring or methylene groups) in the adsorbent structure.[36] The weak peak near 690 cm^{-1} was also attributed to Si—CH_2 stretching bonds and appeared in RC1000-M0.24 and RC1000-M0.48.[24] Also, the peaks at 2361, 896, and 470 cm^{-1} are related to the S—H, Si—OH, and the asymmetric bending of Si—O—C bonds observed in modified samples which become sharper with increasing *M*/*R* ratio.[25,37] Thus, the results of FTIR spectra prove a successful modification of the RF xerogels.

Porous Properties. The porous properties of the xerogels were evaluated by nitrogen physisorption at −196°C. The nitrogen adsorption–desorption isotherms of RC50-M0.24, RC1000-Pure, RC1000-M0.24, and RC1000-M0.72 are shown in Figure 3(a). RC1000-Pure and RC1000-M0.24 show a type IV isotherm with a type H2 hysteresis according to the IUPAC classification which suggests that xerogels are mesoporous and contain a small number of micropores.[38] The nitrogen adsorption–desorption isotherm of RC50-M0.24 is a combination of a type I isotherm, for a microporous solid, and a type II isotherm for a macroporous solid which shows that using the lower *R*/*C* molar ratio causes a sharp increase in the adsorbed nitrogen volume and indicates the existence of a high volume of macropores. However, RC1000-M0.72 can be classified as type I which verifies there is a large portion of micropore volume in the sample. Pore size distributions of the four typical xerogels are depicted in Figure 3(b). It can be seen that the xerogels do not contain a narrow pore size distribution. PSD in RC1000-M0.72 is mainly ranged lower than 4 nm and in RC50-M0.24 is mostly ranged in the upper than 20 nm range. Using more catalyst and MPTMS causes smaller pores and vice versa.

Table II shows the initial gels pH along with the quantitative results derived from the nitrogen adsorption–desorption isotherms. As shown in the table, at the same resorcinol-to-MPTMS (*M*/*R*) molar ratio, the initial pH of RF solutions was decreased by decreasing the resorcinol-to-catalyst (*R*/*C*) molar ratio and reduced from 5.95 for RC1000-M0.24 to 4.62 for RC50-M0.24. In fact, since $MgSO_4{\cdot}7H_2O$ is a weak acidic catalyst, the initial pH is decreased by increasing the amount of catalyst. The variations of *R*/*C* molar ratio and thereby initial pH values make different porous properties. By decreasing the *R*/*C* value in RF solutions, the total pore volume (V_{total}) and the mean pore diameter (d_{mean}) increase, while the BET-specific surface area (S_{BET}) is clearly decreased. The reduction of

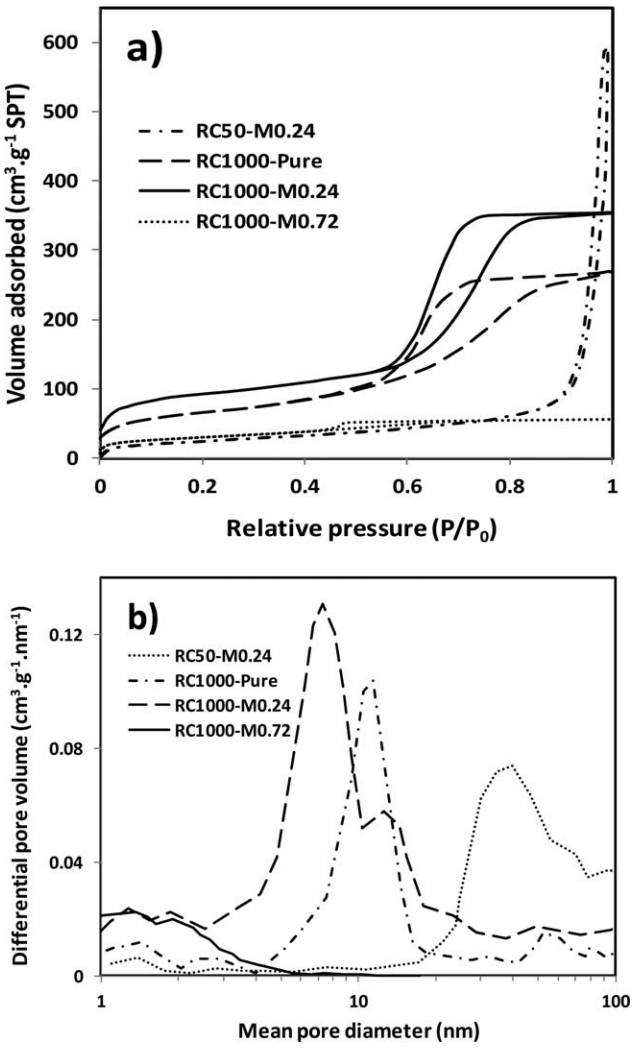

Figure 3. (a) N2 adsorption–desorption isotherms and (b) pore size distributions for RC50-M0.24, RC1000-Pure, RC1000-M0.24, and RC1000-M0.72.

Table II. Textural Properties of Unmodified and Modified Xerogels

Sample	S_{BET} (m^2 g^{-1})[a]	V_{total} (cm^3 g^{-1})[b]	V_{mes} (cm^3 g^{-1})	V_{mic} (cm^3 g^{-1})	V_{mes} (%)[c]	V_{mic} (%)[d]	d_{mean} (nm)[e]	pH
RC50-M0.24	107	1.05	0.31	0.01	29.52	0.95	45.3	4.62
RC200-M0.24	155	0.86	0.51	0.08	59.30	9.30	24.8	5.38
RC600-M0.24	251	0.75	0.54	0.11	72.00	14.66	12.6	5.71
RC1000-M0.24[f]	311	0.69	0.56	0.13	81.44	18.55	8.4	5.98
RC1000-Pure	228	0.59	0.51	0.04	86.44	6.77	12.7	6.52
RC1000-M0.12	290	0.63	0.53	0.08	84.12	12.69	9.5	6.21
RC1000-M0.24[f]	311	0.69	0.56	0.13	81.45	18.55	8.4	5.98
RC1000-M0.48	232	0.42	0.26	0.16	61.91	38.09	6.6	5.51
RC1000-M0.72	87	0.09	0.04	0.05	44.45	55.55	1.8	5.05

[a] BET specific surface area.
[b] V_{total} was obtained from the adsorbed N_2 volume at $P/P_0 = 0.99$.
[c] Mesopore volume percentage.
[d] Micropore volume percentage.
[e] Mean pore diameter.
[f] Same sample.

mesopore and micropore volume percentages (V_{mes} (%) and V_{mic} (%)), and the comparison of their summation with V_{total} leads one to conclude that macropore volume has increased in xerogels, especially in sample RC50-M0.24. This trend can be explained by the chemistry of RF gels during the synthesis. At lower initial pHs, the concentration of resorcinol anions decreases which diminishes the formation of hydroxymethyl derivatives. The less branched system persists longer in the nucleation regime, leading to the larger particles.[8] Finally, it can be seen that RC1000-M0.24 has the maximum S_{BET}, V_{mes}, and V_{mic}. Therefore, the value of $R/C = 1000$ is selected to study the modifier effects on the porous properties of the xerogels. It should be noted that the values of RC50-M0.24 may not be accurate because of a high macropore volume increase in the sample.[19,39]

According to Table II, the initial pH of the RF solution in the absence of MPTMS, i.e., sample RC1000-Pure, is 6.52 and by introducing the modifier to the RF solution, the initial pH is reduced for the samples which indicates that MPTMS has an acidic nature. First, by adding MPTMS to the RF solution, S_{BET} is raised from the value 228 m^2 g^{-1} (RC1000-Pure) to the value 311 m^2 g^{-1} (RC1000-M0.24). However, for the higher doses of MPTMS ($M/R > 0.24$), S_{BET} and V_{mes} decreased. As a matter of fact, the addition of MPTMS causes a portion of the pore volume to be occupied by the mercaptopropyl groups that initially increase surface area, but extra modifier exhibits contrary results for S_{BET}. The excess co-condensation of hydrolyzed silanol groups forms siloxane linkages and hence meso and macropore volumes are occupied and decreased. Thereupon, V_{total} and S_{BET} are extremely decreased. The formation of siloxane linkages and pore occupation are the reason of increasing and decreasing V_{mic} (%) and d_{mean} while raising the M/R ratio in xerogels, respectively. It can be concluded from the information above that RC1000-M0.24 has the highest specific surface area and mesopore volume among the others. It should also be noted that the effect of organosilane polymerization on porous properties is found to be more dominant compared to the initial pH effect.

Scanning Electron Microscopy (SEM). SEM micrographs of the surface morphology of RC50-M0.24, RC600-M0.24, RC1000-Pure, and RC1000-M0.24 are shown in Figures 4 and 5. As can be observed in Figure 4(a), RC50-M0.24 mainly contains large particles which result in broad interparticle voids while in RC600-M0.24 [Figure 4(b)], the particles appear finer. The recent comparison indicates substantial effects of R/C variation on the xerogels morphology at the same M/R ratio which basically relates to the initial pH effect. In fact, the low pH value of the RF gel results in large colloidal particles and on the contrary higher pH value causes small particles. Furthermore, the effect of M/R ratio could be realized from the morphology of RC1000-Pure (Figure 5a) and RC1000-M0.24 (Figure 5b). With increasing M/R ratio from 0 to 0.24 at a fixed value of $R/C = 1000$, the particle size is obviously decreased and the fused particle morphology has become more smooth and homogeneous.

Thermal Analysis. In Figure 6, TG–DTG curves for xerogels RC1000-Pure and RC1000-M0.24 are shown. As can be seen from the figure, the weight loss of RC1000-M0.24 is lower than that of RC1000-Pure over all the temperatures. The total weight loss of RC1000-Pure and RC1000-M0.24 are measured to be 56.5 and 48.7% during pyrolysis in N_2, respectively. The differential thermogravimetric (DTG) curve of RC1000-Pure shows three peaks at 120, 415, and 602°C. The first peak at 120°C with about 4% weight loss is related to the physical desorption of the residual solvent in the xerogel. The peaks at 415 and 602°C are attributed to the carbonization reactions and breaking C—O and C—H bonds, respectively.[14] These reactions start around 305°C and end at 850°C with a major weight loss of 48%. A similar trend is observed from the DTG curve of RC1000-M0.24. However, RC1000-M0.24 shows an additional peak at 372°C which can be explained by the decomposition of the mercapto groups.[40] The higher thermal stability of RC1000-M0.24

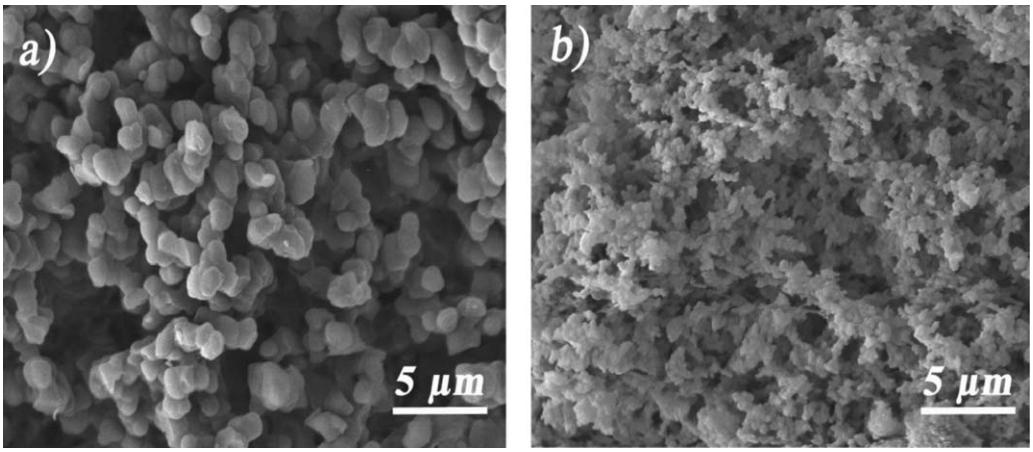

Figure 4. SEM micrographs of (a) RC50-M0.24 and (b) RC600-M0.24.

is due to the participation of silane bonds, such as Si—O and Si—O—Si, in the chemical structure of the modified xerogel.

Adsorption Study of Mercury

Effect of Reagents. The adsorption experiments for all the synthesized xerogels are performed at the initial Hg(II) ions concentration of 50 mg L^{-1} for a 1.5 g L^{-1} adsorbent dose, pH 6, and a contact time of 120 min.

The mercury adsorption efficiency (E) and surface area (S_{BET}) of the samples are shown against the R/C molar ratio in Figure 7 for the xerogels with $M/R = 0.24$. From the figure, the trend of adsorption variation is similar to the trend of surface area change and both of E and S_{BET} are increased with increasing R/C ratio. In fact, E is related to the value of S_{BET}. As pore surface area increases more adsorption sites such as thiol groups are available for Hg(II) ions. The highest E value is related to RC1000-M0.24 (at $R/C = 1000$) possesses $S_{BET} = 311$ m^2 g^{-1}.

The change in mercury adsorption efficiency and surface area versus the M/R molar ratio can be seen in Figure 8. As can be seen from the figure, both E and S_{BET} have maximum values in $M/R = 0.24$ meanwhile the trends of change indicate a correlation between E and S_{BET}. The extra amount of MPTMS, i.e., $M/R > 0.24$, causes more silanol groups to polycondensate with each other and form more siloxane linkages that in turn result in the lower adsorption of Hg(II) ions. From Figure 8, it can be shown that the effect of the amount of MPTMS, in the formula, on adsorption efficiency is higher than the surface area of the xerogel as RC1000-Pure ($M/R = 0$) possesses higher S_{BET} than RC1000-M0.72 (at $M/R = 0.72$) while it shows a lower adsorption. Also RC1000-M0.48 ($M/R = 0.48$) has a greater adsorption efficiency value than RC1000-M0.12 ($M/R = 0.12$) while it possesses lower S_{BET}. The domination of chemical modification leads to the presence of mercapto groups on the pore surface and thereby the high affinity and selectivity for Hg(II) by —SH groups.

Ultimately, from the adsorption results in Figures 7 and 8, it can be said that RC1000-M0.24 has the highest surface area and is the best mercury adsorbent among the synthesized RF xerogels. So, RC1000-M0.24 is the optimized mercapto-modified xerogel used for studying the pH effect and also adsorption isotherm and kinetics.

Effect of pH. The pH of a metal ion solution is an important parameter in adsorption process because it affects the solubility of the metal ions, concentration of the counter ions on the functional groups of the adsorbent, and the degree of ionization of the adsorbate.[41] The pH value also controls the complexation reactions or electrostatic interactions in the physisorption processes at the adsorption surface.[42] Thus, the effect of pH on the adsorption efficiency xerogels is studied at two different initial

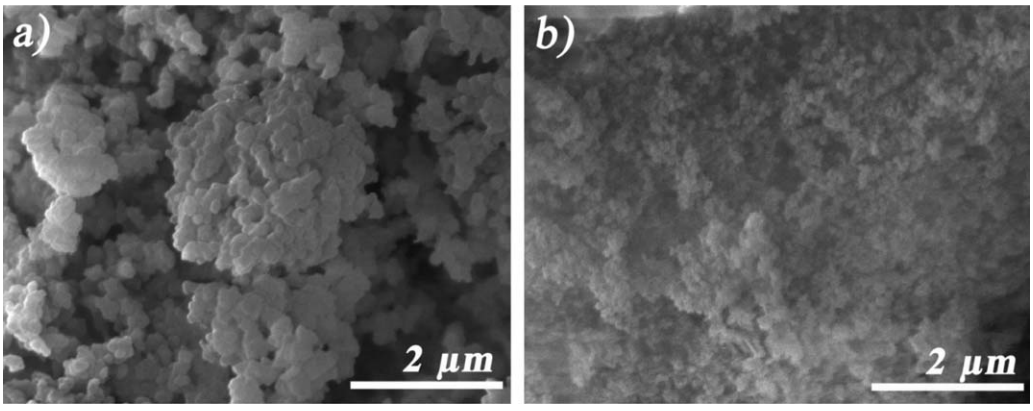

Figure 5. SEM micrographs of RF xerogels: (a) RC1000-Pure (b) RC1000-M0.24.

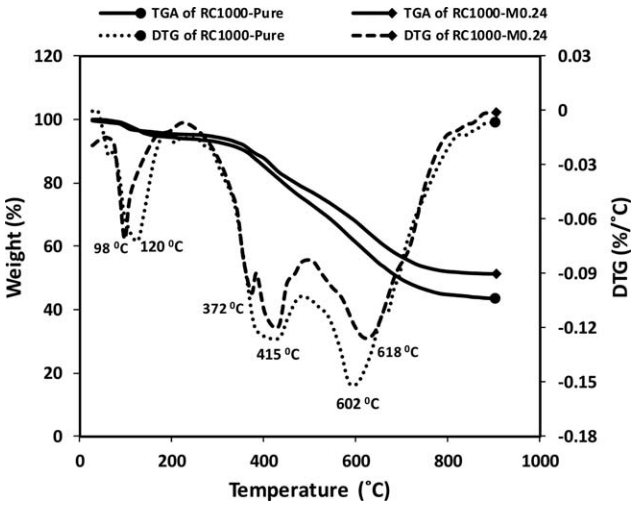

Figure 6. TG–DTG curves of RC1000-Pure and RC1000-M0.24 xerogels.

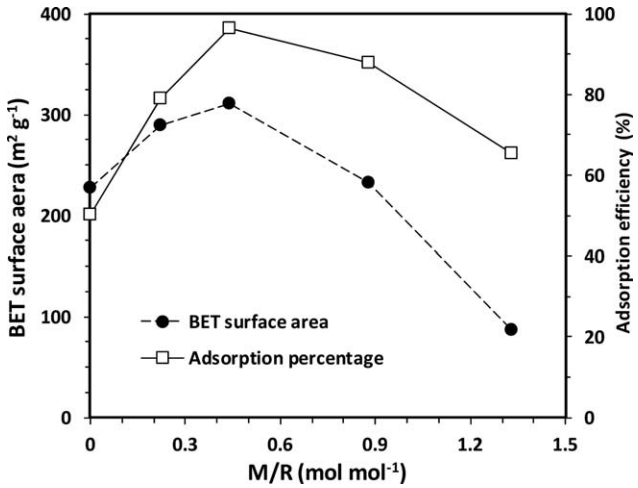

Figure 8. Effect of *M/R* molar ratio on mercury adsorption efficiency and BET surface area with *R/C* = 1000.

Hg(II) concentrations for RC1000-M0.24 and at one initial Hg(II) concentration for RC1000-Pure as presented in Figure 9. For all experiments, the adsorbents dose, contact time, and the solution temperature are chosen to be 1.5 g L^{-1}, 2 h, and 25°C, respectively. The pH is adjusted by dilute HCl or NaOH solutions for the range 2–8.

The findings indicate that the Hg(II) removal is increased by increasing the pH value and then reaches a plateau after pH 5 for both RC1000-M0.24 and RC1000-Pure. This behavior can be explained by the ion-exchange mechanism at the adsorbent surface. At low pH values, Hg(II) ions exist in the form of Hg^{2+} that compete with the high concentration of H^+ ions to be adsorbed at the ion-exchangeable sites. In addition, the positive charge of the adsorbent and Hg(II) ions at low pH values cause an extensive electrostatic repulsion interaction among them. Thus, low adsorption efficiency is expected under acidic solution conditions. The increase in Hg(II) adsorption with the increasing of pH can be explained on the basis of a reduction in the proton concentration and therewith the decrease in competition between the H^+ ions and Hg(II) species for the same adsorbent surface. On the other side, the presence of different Hg(II) species (i.e., Hg^{2+}, $HgOH^+$, $Hg(OH)_2$) in the adsorption medium is extremely dependent on the pH value; at higher pH values, the Hg(II) species present in the form of $HgOH^+$ and $Hg(OH)_2$, so the electrostatic repulsion among the adsorbent functional groups and Hg(II) species decreases significantly. The trend of the removal changes for RC1000-Pure is obviously more than RC1000-M0.24 that shows RC1000-M0.24 has a high adsorption capacity even at low pH values. The high capacity of RC1000-M0.24 is due to the presence of mercapto groups on the pore surface and thereby the high affinity and selectivity of —SH groups toward Hg(II) species.

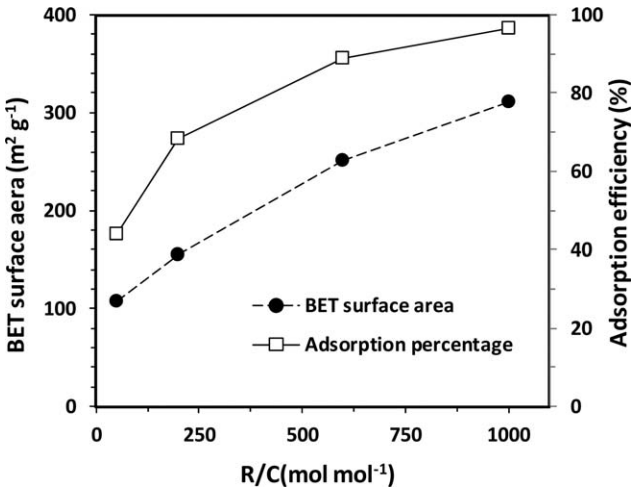

Figure 7. Effect of *R/C* molar ratio on mercury adsorption efficiency and BET surface area of samples with *M/R* = 0.24.

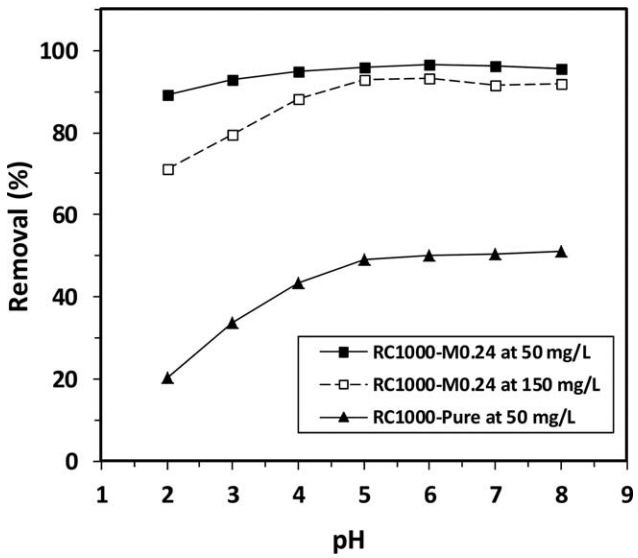

Figure 9. Effect of pH on Hg(II) adsorption for RC1000-Pure and RC1000-M0.24 (■: adsorption data for RC1000-M0.24 at 50 mg L^{-1} of initial concentration; □: adsorption data for RC1000-M0.24 at 150 mg L^{-1} of initial concentration; ▲: adsorption data for RC1000-Pure at 50 mg L^{-1} of initial concentration).

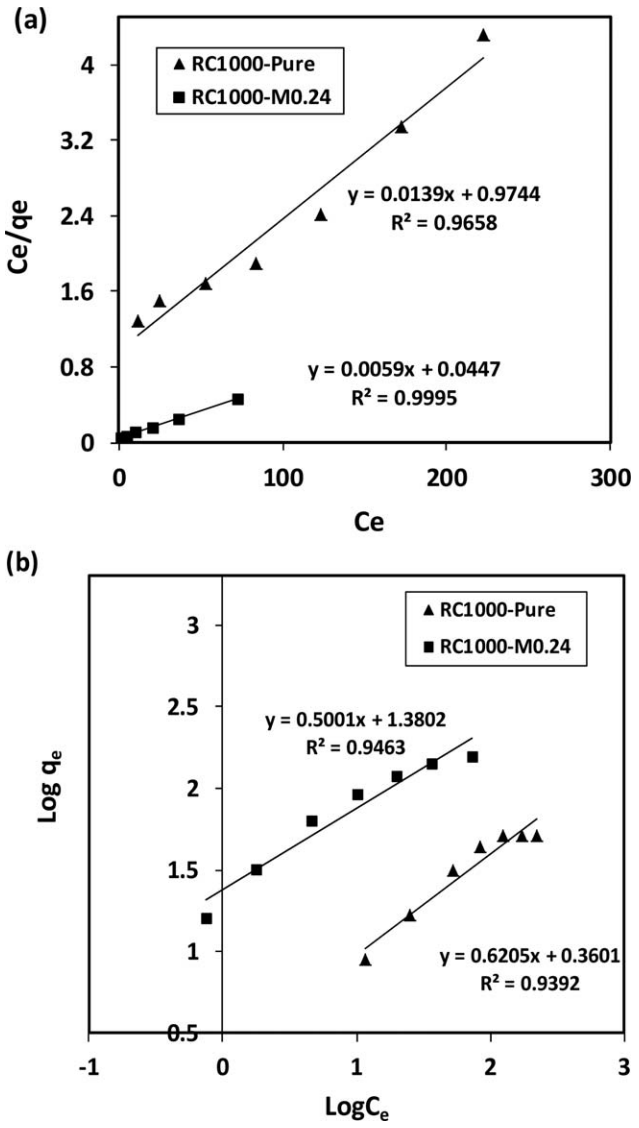

Figure 10. (a) Langmuir isotherm and (b) Freundlich isotherm for adsorption of Hg(II) on RC1000-Pure and RC1000-M0.24.

When the initial concentration of Hg increases from 50 to 150 mg L^{-1}, the pH shows to be more effective on the adsorption of RC1000-M0.24 in the lower values. This could be due to the fact that there are more Hg(II) species in the solution, so that there are less available active sites (—SH) left and thereby more competition takes place.[43] Some similar adsorption patterns are reported in accordance with the present results.[32,43–45]

Adsorption Isotherms. Adsorption isotherm plays an important role in describing the solute–adsorbent interaction and defines the optimized amount of the adsorbent which should be used. The study of the adsorption isotherm is carried out by using different initial Hg(II) concentration ranges from 25 to 300 mg L^{-1} for fixed adsorbent dose of 1.5 g L^{-1}. The adsorption data is fitted with Langmuir and Freundlich isotherm models.

The isothermal adsorption data is fitted to Langmuir and Freundlich isotherm models which are shown in Figure 10(a,b) and the obtained isotherm constants are regrouped in Table III. The correlation coefficients (R^2) indicate that the adsorption data of Hg(II) on both RC1000-Pure and RC1000-M0.24 samples can be fitted more accurately by the Langmuir isotherm compared to the Freundlich isotherm. The R_L values for RC1000-Pure and RC1000-M0.24 are also found to be 0.192 and 0.024, which confirm that both of the xerogels are favorable for the adsorption of Hg(II) under conditions used in this study. In the Freundlich isotherm model, the value of $1/n$ is between 0 and 1 which indicates a favorable adsorption. The adsorption becomes more intensive and heterogeneous when $1/n$ value approaches zero.[43,46] As can be seen in Table III, the $1/n$ value is less for RC1000-M0.24 as compared to that of RC1000-Pure and at the same time, the K_F value is much higher for RC1000-M0.24 compared to that of RC1000-Pure. Thus it can be concluded that RC1000-M0.24 has a higher adsorption capacity and intensity for Hg(II) ions than RC1000-Pure.[43] The correlation coefficient values (R^2) for RC1000-M0.24 are also higher than that of RC1000-Pure in both the isotherms which indicate the adsorption process occurs more favorably by RC1000-M0.24. However, the Langmuir isotherm models the process better than the Freundlich isotherm does.

In conclusion, both Freundlich and Langmuir isotherms confirm higher adsorption affinity of RC1000-M0.24 for Hg(II) ions compared to RC1000-Pure. Table IV presents a comparison of the values of Hg(II) monolayer adsorption capacity, q_m (mg g^{-1}), obtained from the Langmuir model, for RC1000-M0.24 and other synthesized adsorbents. The comparison shows that the present modified RF xerogel can be an effective Hg(II) adsorbent for wastewater treatment. In addition, considering the low cost and easy production of RC1000-M0.24, it is a very promising industrial adsorbent for the removal of Hg(II) ions.

Adsorption Kinetics. For the first- and second-order kinetic models, the experimental data are evaluated by the linear plots of log ($q_e - q_t$) *vs* t and (t/q_t) *vs* t, respectively, as shown in Figure 11(a,b). The experimental data which are collected at various contact times up to 240 min are compared to the kinetic models. Using linear regressions, the kinetic parameters are calculated from the slope and the intercept of the plots which are represented in Table V. As can be seen in Table V, adsorption data for both RC1000-Pure and RC1000-M0.24 are more in

Table III. Freundlich and Langmuir Isotherm Constants for Adsorption of Hg(II)

	Langmuir isotherm				*Freundlich isotherm*		
	q_m	K_L	R_L	R^2	K_F	$1/n$	R^2
RC1000-Pure	71.94	0.014	0.192	0.9658	2.3	0.62	0.9392
RC1000-M0.24	169.49	0.131	0.024	0.9995	24	0.50	0.9463

Table IV. Comparison of Monolayer Adsorption Capacity of Hg(II) for Various Adsorbents Obtained from Langmuir Model

Adsorbent type	Active sites	q_m (mg/g)	Reference
Activated carbon (from *Bambusa vulgaris striata*)	—COOH, —CO—	248.05	47
Modified silica aerogel	—SH, —OH	181.81	25
Modified RF xerogel	—SH, —OH	169.49	This study
Mesoporous silica nanocomposite	—SH, —C—NH—C—, —OH	163.93	48
Modified wool fibers	—CN, —NH_2, —CO—NH—	154.32	49
Activated carbon (from agricultural wastes)	—COOH, —OH, —COO—	147.1	5
Modified multiwalled carbon nanotubes	—OH, —COOH	32.4-127.6	50
Carbon aerogel	—OH, —COOH	45.62	3
Modified Egyptian mandarin peel	—OH, —COOH	34.84	51
Polyacrylamide aerogel	—CO—NH_2	13.21-17.63	10
Silica aerogel	—OH	4.42-11.60	10
Hybrid aerogel	—CO—NH_2, —OH	8.39-13.69	10

accordance with the pseudo-second-order model since the correlation coefficient, R^2, is closer to 1. Furthermore, to choose the proper model, the calculated adsorption capacity value of Hg(II) at equilibrium, $q_{e(theory)}$, should be close to the experimental $q_{e(experimental)}$ value.[52] The experimental adsorption capacities of RC1000-Pure ($q_{e(experimental)} = 19.66$ mg g^{-1}) and RC1000-M0.24 ($q_{e(experimental)} = 33.33$ mg g^{-1}) show a good agreement with theoretical q_e values ($q_{e(theory)}$) of the pseudo-second-order model. These results suggest that the adsorption of Hg(II) ions on the xerogels is not a first-order reaction and follows the second-order-type kinetic reaction. So the adsorption process involves chemisorption in addition to the physisorption mechanism. The chemisorption might be the rate-limiting step which probably occur via complexation and/or chelation between —OH in RC1000-Pure and —OH and —SH in RC1000-M0.24 functional groups and Hg(II) ions.

Desorption of Hg(II) and Reusability of Adsorbent

To study the desorption performance and reusability of modified RF xerogel, the same RC1000-M0.24 sample is used five times in adsorption–desorption cycles. During those adsorption–desorption cycles, the adsorbent dose has been 1.5 g L^{-1}. The desorption is performed using HCl at a concentration of 3 M containing 2% (m/v) thiourea as an optimized eluent which is already applied by Othman Hakami *et al.*[32] for recovery of Hg(II) from water through a kind of thiol-functionalized mesoporous adsorbent. It should be noted that all adsorption experiments were carried out with the adsorbent dose of 1.5 g L^{-1}, initial Hg(II) ions concentration of 50 mg L^{-1}, a pH 6, and a contact time of 2 h. The results of the adsorption efficiency and the desorption ratio of RC1000-M0.24 for five adsorption–desorption cycles are shown in Figure 12. As previously defined, the desorption ratio expresses the desorption percentage of what is already adsorbed. The results indicate that both adsorption efficiency and desorption ratio of Hg(II) decrease by increasing the adsorption–desorption cycles. These reductions might be due to the fact that Hg(II) ions are not completely released from the adsorption sites among recovery cycles and the —S—Hg bonds are stable, thereby some adsorption sites are deactivated. It can also be seen from Figure 8 that

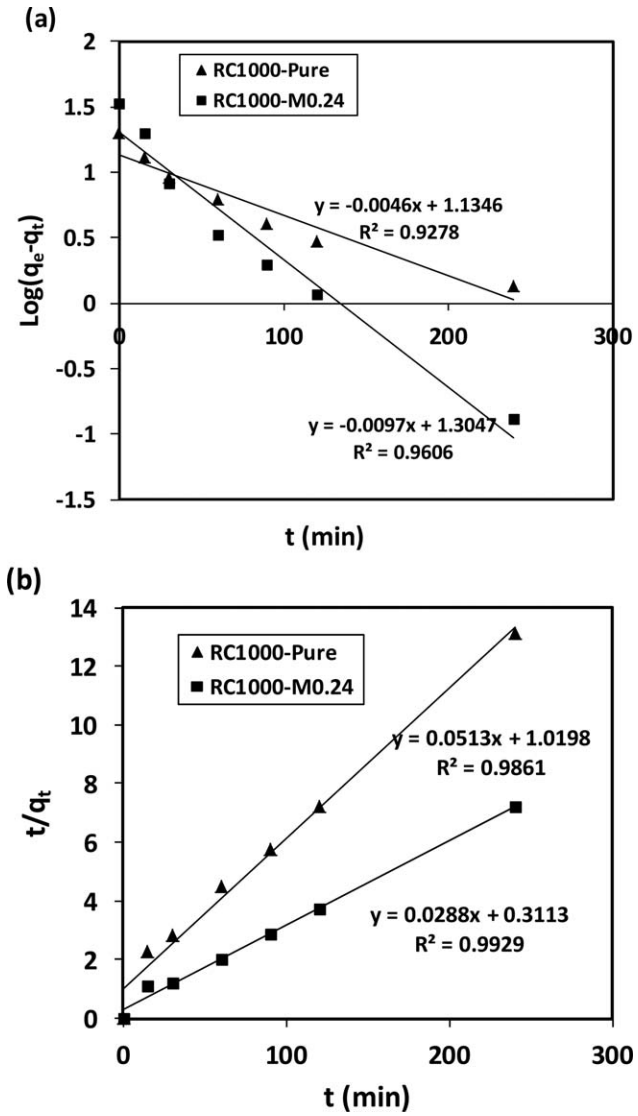

Figure 11. The (a) pseudo-first-order kinetic plots and (b) the pseudo-second-order kinetic plots for adsorption of Hg(II) on RC1000-Pure and RC1000-M0.24.

Table V. Adsorption Kinetic Constants for Adsorption of Hg(II)

		Pseudo-first-order			Pseudo-second-order		
	$q_{e\ (experimental)}$	$q_{e\ (theory)}$	k_1	R^2	$q_{e\ (theory)}$	k_2	R^2
RC1000-Pure	19.66	13.63	0.0105	0.9278	19.49	0.00258	0.9861
RC1000-M0.24	33.33	20.17	0.0223	0.9606	34.72	0.00266	0.9929

the adsorption percentage from first cycle to fifth cycle is decreased from 96.5 to 83.2%. This slight reduction is indebted to the stable mercapto functional groups in the modified xerogel structure.

CONCLUSION

In this study, RF xerogels modified with mercapto functional groups are synthesized to be used as a mercury adsorbent. The amounts of catalyst and MPTMS in RF solution are varied to optimize the physical and chemical properties of the pore structure. FTIR spectra proved a successful modification of the RF xerogels. The results of nitrogen adsorption–desorption indicate that the *R/C* and *M/R* ratios drastically altered the pore texture due to the variation of the initial gels pH and pore occupation, respectively. SEM micrographs demonstrated that the *R/C* and *M/R* ratio can also control the surface morphology of the xerogels. Furthermore, the participation of silane bonds, such as Si—O and Si—O—Si, in the chemical structure of the modified xerogel causes a higher thermal stability compared to the unmodified one. For evaluating the mercury adsorption performance of the xerogels, a series of adsorption tests are carried out under certain predetermined conditions. The experimental measurements show adsorption efficiency is affected by both the chemical modification and surface area of the absorbent simultaneously. Sample RC1000-M0.24 adsorbed the highest amount of mercury ion which also has the highest surface area compared to the other modified RF xerogels. The effect of pH is also studied on the adsorption performance of both the modified and unmodified samples. The results indicate that the Hg(II) removal is increased by increasing the pH value and then reaches a plateau after pH 5 for both the xerogels. Furthermore, the adsorption isotherm, kinetics, and mechanism are studied too. Adsorption data can be fitted well to the Langmuir and Freundlich isotherm equations and also are suitably modeled by the pseudo-second-order kinetics model. After five cycles of adsorption–desorption, the adsorption efficiency is not reduced considerably which is indebted to the stable mercapto functional groups in the modified RF xerogel structure. This study suggests that the optimized modified RF xerogels are quite suitable for mercury adsorption in industrial applications.

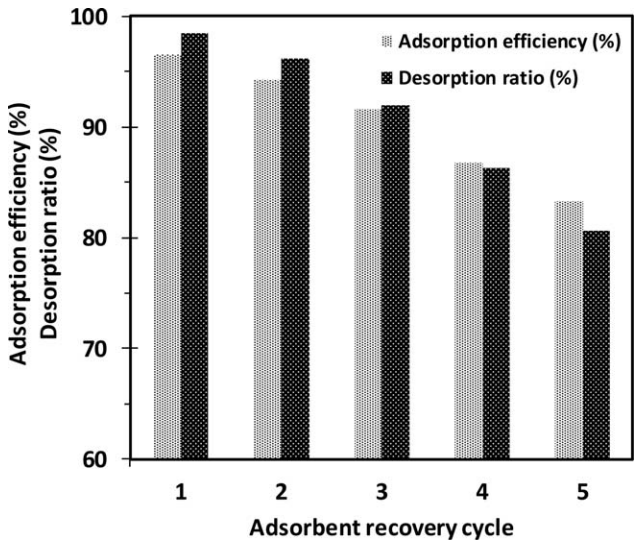

Figure 12. Adsorption efficiency and desorption ratio of Hg(II) for different RC1000-M0.24 recovery cycles.

REFERENCES

1. Keith, L.; Telliard, W. *Environ. Sci. Technol.* **1979**, *13*(4), 416.
2. Directive, W. F. Web source: http://eur-lex europa eu/ LexUriServ/LexUriServ do? uri= OJ: L: 2000: 327: 0001 2000, 72.
3. Meena, A. K.; Mishra, G.; Rai, P.; Rajagopal, C.; Nagar, P. *J. Hazard. Mater.* **2005**, *122*(1), 161.
4. Touaibia, D.; Benayada, B. *Desalination* **2005**, *186*(1), 75.
5. Asasian, N.; Kaghazchi, T.; Soleimani, M. *J. Ind. Eng. Chem.* **2012**, *18*(1), 283.
6. Asasian, N.; Kaghazchi, T.; Faramarzi, A.; Hakimi-Siboni, A.; Asadi-Kesheh, R.; Kavand, M.; Mohtashami, S.-A. *J. Taiwan Inst. Chem. Eng.* **2014**, *45*(4), 1588.
7. Moreno-Castilla, C.; Maldonado-Hódar, F. *Carbon* **2005**, *43*(3), 455.
8. Aegerter, M. A.; Leventis, N.; Koebel, M. M. Aerogels Handbook, Springer Science & Business Media, **2011**.
9. Liu, H.; Sha, W.; Cooper, A. T.; Fan, M. *Colloids Surf. A: Physicochem. Eng. Asp.* **2009**, *347*(1), 38.
10. Ramadan, H.; Ghanem, A.; El-Rassy, H. *Chem. Eng. J.* **2010**, *159*(1), 107.
11. Awadallah-F, A.; Elkhatat, A. M.; Al-Muhtaseb, S. A. *J. Mater. Sci.* **2011**, *46*(24), 7760.
12. Kocklenberg, R.; Mathieu, B.; Blacher, S.; Pirard, R.; Pirard, J.-P.; Sobry, R.; Van den Bossche, G. *J. Non-Cryst. Solids* **1998**, *225*, 8.
13. Hwang, S.-W.; Hyun, S.-H. *J. Non-Cryst. Solids* **2004**, *347*(1), 238.
14. Sharma, C. S.; Kulkarni, M. M.; Sharma, A.; Madou, M. *Chem. Eng. Sci.* **2009**, *64*(7), 1536.
15. Al-Muhtaseb, S. A.; Ritter, J. A. *Adv. Mater.* **2003**, *15*(2), 101.

16. Yamamoto, T.; Nishimura, T.; Suzuki, T.; Tamon, H. *J. Non-Cryst. Solids* **2001**, *288*(1), 46.
17. Sharma, C. S.; Upadhyay, D. K.; Sharma, A. *Ind. Eng. Chem. Res.* **2009**, *48*(17), 8030.
18. ElKhatat, A. M.; Al-Muhtaseb, S. A. *Adv. Mater.* **2011**, *23*(26), 2887.
19. Job, N.; Pirard, R.; Marien, J.; Pirard, J.-P. *Carbon* **2004**, *42*(3), 619.
20. Lin, C.; Ritter, J. *Carbon* **1997**, *35*(9), 1271.
21. Manzano, M.; Aina, V.; Arean, C.; Balas, F.; Cauda, V.; Colilla, M.; Delgado, M.; Vallet-Regi, M. *Chem. Eng. J.* **2008**, *137*(1), 30.
22. Arencibia, A.; Aguado, J.; Arsuaga, J. M. *Appl. Surf. Sci.* **2010**, *256*(17), 5453.
23. Walcarius, A.; Delacôte, C. *Analytica Chimica Acta* **2005**, *547*(1), 3.
24. Idris, S. A.; Harvey, S. R.; Gibson, L. T. *J. Hazard. Mater.* **2011**, *193*, 171.
25. Štandeker, S.; Veronovski, A.; Novak, Z.; Knez, Ž. *Desalination* **2011**, *269*(1), 223.
26. Faghihian, H.; Nourmoradi, H.; Shokouhi, M. *Polish J. Chem. Technol.* **2012**, *14*(1), 50.
27. Pekala, R. *J. Mater. Sci.* **1989**, *24*(9), 3221.
28. Brunauer, S.; Emmett, P. H.; Teller, E. *J. Am. Chem. Soc.* **1938**, *60*(2), 309.
29. Mikhail, R. S.; Brunauer, S.; Bodor, E. *J. Colloid Interface Sci.* **1968**, *26*(1), 45.
30. Barrett, E. P.; Joyner, L. G.; Halenda, P. P. *J. Am. Chem. Soc.* **1951**, *73*(1), 373.
31. Chowdhury, S.; Mishra, R.; Saha, P.; Kushwaha, P. *Desalination* **2011**, *265*(1), 159.
32. Hakami, O.; Zhang, Y.; Banks, C. *J. Water Res.* **2012**, *46*(12), 3913.
33. Foo, K.; Hameed, B. *Chem. Eng. J.* **2010**, *156*(1), 2.
34. Hameed, B.; Din, A. M.; Ahmad, A. *J. Hazard. Mater.* **2007**, *141*(3), 819.
35. Velikova, N.; Vueva, Y.; Ivanova, Y.; Salvado, I.; Fernandes, M.; Vassileva, P.; Georgieva, R.; Detcheva, A. *J. Non-Cryst. Solids* **2013**, *378*, 89.
36. Demjen, Z.; Pukanszky, B.; Nagy, Jr, J. *Polymer* **1999**, *40*(7), 1763.
37. Gwon, J. G.; Lee, S. Y.; Doh, G. H.; Kim, J. H. *J. Appl. Polym. Sci.* **2010**, *116*(6), 3212.
38. Sing, K. S. *Pure Appl. Chem.* **1985**, *57*(4), 603.
39. Haghgoo, M.; Yousefi, A. A.; Mehr, M. J. Z. *Iran. Polym. J.* **2012**, *21*(4), 211.
40. Möller, K.; Kobler, J.; Bein, T. *J. Mater. Chem.* **2007**, *17*(7), 624.
41. Zvinowanda, C.; Okonkwo, J.; Shabalala, P.; Agyei, N. *Int. J. Environ. Sci. Technol.* **2009**, *6*(3), 425.
42. Ünlü, N.; Ersoz, M. *J. Hazard. Mater.* **2006**, *136*(2), 272.
43. Pan, S.; Shen, H.; Xu, Q.; Luo, J.; Hu, M. *J. Colloid Interface Sci.* **2012**, *365*(1), 204.
44. Goel, J.; Kadirvelu, K.; Rajagopal, C.; Garg, V. K. *J. Chem. Technol. Biotechnol.* **2005**, *80*(4), 469.
45. Wang, J.; Deng, B.; Wang, X.; Zheng, J. *Environ. Eng. Sci.* **2009**, *26*(12), 1693.
46. Acharya, J.; Sahu, J.; Mohanty, C.; Meikap, B. *Chem. Eng. J.* **2009**, *149*(1), 249.
47. González, P.; Pliego-Cuervo, Y. *Chem. Eng. Res. Des.* **2014**.
48. Javadian, H.; Taghavi, M. *Appl. Surf. Sci.* **2014**, *289*, 487.
49. Monier, M.; Nawar, N.; Abdel-Latif, D. *J. Hazard. Mater.* **2010**, *184*(1), 118.
50. Chen, P. H.; Hsu, C.-F.; Tsai, D. D.-W.; Lu, Y.-M.; Huang, W.-J. *Environ. Technol.* **2014**, *35*(15), 1935.
51. Husein, D. Z. *Desal. Water Treat.* **2013**, *51*(34–36), 6761.
52. Ho, Y.; McKay, G. *Process Saf. Environ. Prot.* **1998**, *76*(4), 332.